Applied Catalysis B: Environmental 97 (2010) 340–346

Contents lists available at ScienceDirect

Applied Catalysis B: Environmental

journal homepage: www.elsevier.com/locate/apcatb

Surface acidity and reactivity of β-FeOOH/Al_2O_3 for pharmaceuticals degradation with ozone: In situ ATR-FTIR studies

Li Yang, Chun Hu*, Yulun Nie, Jiuhui Qu

State Key Laboratory of Environmental Aquatic Chemistry, Research Center for Eco-Environmental Sciences, Chinese Academy of Sciences, Beijing 100085, China

ARTICLE INFO

Article history:
Received 14 December 2009
Received in revised form 10 April 2010
Accepted 13 April 2010
Available online 22 April 2010

Keywords:
ATR-FTIR
Catalytic ozonation
Mesoporous alumina
β-FeOOH
Pharmaceuticals
Surface Lewis acid sites

ABSTRACT

The surface acidity and reactive activity of β-FeOOH, mesoporous alumina (MA), β-FeOOH/MA were investigated in catalytic ozonation of pharmaceutically active compounds (PhACs) aqueous solution. β-FeOOH/MA showed high efficiency for the degradation and mineralization of ibuprofen and ciprofloxacin. Its surface Lewis acid sites on β-FeOOH/MA were more greatly enhanced compared with those on MA and β-FeOOH. In situ attenuated total reflection FTIR (ATR-FTIR) spectroscopy was used to investigate the interaction of D_2O and O_3 with the catalysts in aqueous phase under various conditions. The dissociative chemisorptions of D_2O occurred at the surface Lewis acid sites of the catalyst. Furthermore, O_3 interacted with the surface hydrogen-bonded –O–D and D_2O to initiate reactive oxygen species (ROS). The stronger Lewis acid sites of β-FeOOH/MA caused the more chemisorbed water enhancing the interaction with ozone, resulting in higher catalytic reactivity. The observations verified that the Lewis acid sites were reactive centers for the catalytic ozonation of PhACs in water.

1. Introduction

In recent years, numerous studies have established the occurrence of pharmaceutically active compounds (PhACs) and several drug metabolites in the aquatic environment [1–4]. Although the detected concentration levels of PhACs in aqueous environment are low and often range from ng/L to μg/L levels, the potential dangers to human and ecological health exist due to long-term exposure [5,6]. PhACs show a wide range of persistence in aquatic environments, and some are highly persistent, which have been found to resist water and wastewater treatment [7,8].

Ozonation and especially advanced oxidation processes seem to be very effective in removal of PhACs [9,10]. However, some PhACs, such as ibuprofen and ciprofloxacin could not be completely degraded with ozone alone [11,12]. Heterogeneous catalytic ozonation has received increasing attention in recent years due to its potentially higher effectiveness in the degradation and mineralization of refractory organic pollutants and lower negative effect on water quality. It has been developed to overcome the limitations of ozonation processes, such as the formation of byproducts and selective reactions of ozone, which are designed to enhance the production of hydroxyl radicals (•OH), known nonselective oxidants [13,14].

Supported and unsupported metals and metal oxides are the most commonly tested catalysts for the ozonation of organic compounds in water or air [15–18]. It has been verified that the catalyst activity for catalytic ozonation mainly depends on its surface acid–base property [18]. Bulanin et al. [19] suggested that ozone dissociates after adsorption on strong Lewis sites yielding a surface oxygen atom, whereas on weaker sites, ozone molecules coordinate via one of the terminal oxygen atoms. This situation takes place in gaseous phase. In aqueous phase, it still could not be confirmed whether ozone adsorption/decomposition occurs on the Lewis acid sites as do in gaseous phase due to the possible interaction of H_2O, OH^- and other hard Lewis bases commonly present in water. There is no evidence to prove whether the Lewis acid sites are active surface sites for the decomposition of O_3 in water. Zhao et al. [20] proposed that molecule ozone in aqueous solution should interact with the surface–OH_2^+ existing on the surface of catalyst according to two basic attractive forces: electrostatic forces or/and hydrogen bonding to initiate the formation of •OH. The surface hydroxyl groups of metal oxides in aqueous solution came from surface hydroxylation of chemisorbed water, which occurred only at the lattice metal ion site acting as a Lewis acid [21–23]. Therefore, the surface Lewis acid sites of the catalyst still played an important role for catalytic ozonation in aqueous phase.

In the present study, the primary objective was to investigate the relationship of both the acid–base properties and the activity of catalysts for catalytic ozonation in water. Mesoporous γ-Al_2O_3 (MA), β-FeOOH and MA-supported β-FeOOH were synthesized and examined for the catalytic ozonation of ibuprofen and ciprofloxacin

* Corresponding author. Tel.: +86 10 62849628; fax: +86 10 62923541.
E-mail address: huchun@rcees.ac.cn (C. Hu).

0926-3373/$ – see front matter © 2010 Elsevier B.V. All rights reserved.
doi:10.1016/j.apcatb.2010.04.014

Table 1
The structure of selected pharmaceuticals.

Name	Chemical structure	pK_a
Ibuprofen	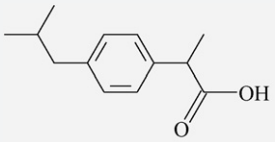	4.9
Ciprofloxacin	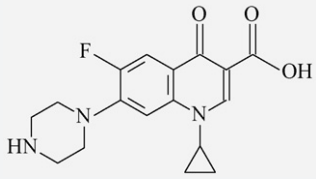	6.27^{-COOH} $8.87^{=NH_2^+}$

in water. The MA-supported β-FeOOH was found to be highly effective for the mineralization of ibuprofen and ciprofloxacin with ozone. The surface acidity and catalytic activity of the catalyst were investigated in detail by in situ ATR-FTIR spectroscopy under different experiments. The results indicate that the Lewis acid sites are crucial surface reactive centers for chemisorbed water molecules, and the active species generated from the interaction of ozone with the surface hydroxyl. It was verified that the Lewis acid sites were catalytic ozonation centers in aqueous phase.

2. Experimental

2.1. Materials and reagents

Ibuprofen (IBU) was obtained from TCI Japan (Tokyo, Japan), and ciprofloxacin (CPFX) was purchased from Acros (Geel, Belgium). Their purities were higher than 99%. Their structure and pK_a were shown in Table 1. Aluminum *i*-propoxide ($Al(O_iPr)_3$), glucose and urea were purchased from Beijing Chemical Reagents (Beijing, China). Iron chloride hexahydrate was acquired from Xilong Chemical Factory (Shantou, China). All the other reagents were analytical grade and used as received. All solutions were prepared with deionized water. The initial pH of the solution was adjusted with HCl or NaOH.

2.2. Catalyst preparation

Mesoporous γ-Al_2O_3 (MA) was prepared from precursors of $Al(O_iPr)_3$ in the presence of glucose in aqueous system according to the reported method [24]. Then β-FeOOH was supported on MA by hydrothermal hydrolysis process with iron chloride hexahydrate ($FeCl_3{\cdot}6H_2O$) as the metal precursor. As an example, 0.30 g of ferric chloride and 0.40 g urea were dissolved in 3 mL of distilled water, and 2 g MA was added to this solution. The pH was adjusted to 1.6 with hydrochloric acid. Subsequently, the temperature was maintained at 373 K with a water bath for 4 h, and then cooled to room temperature naturally and the sample was washed with deionized water. Following this procedure, the catalysts with different Fe contents were prepared from 1 to 8 wt%, while the catalyst with 3 wt% Fe exhibited the highest activity, designated by β-FeOOH/MA, and was used for all of the experiments. The weight percent of Fe was calculated by the ratio of the dosage of Fe to the total dosage of γ-Al_2O_3 and Fe. As reference, the unsupported β-FeOOH was synthesized by the same procedure in the absence of MA.

2.3. Characterization

Nitrogen adsorption/desorption experiments of various samples were carried out using a Micromeritics ASAP2000 analyzer (Micromeritics, Norcross, GA). Powder X-ray diffraction (XRD) of the catalyst was recorded on an XDS-2000 Diffractometer (Scintag, Cupertino, CA) with Cu Kα radiation (λ = 1.54059 Å). The zeta potential of catalysts in the KNO_3 (10^{-3} M) solution was measured with a Zetasizer 2000 (Malvern, Worcestershire, UK) with three consistent readings. The preparation processes of ozonated samples for FTIR analysis were as follows. A desired amount of catalyst particles was added into water, followed by the addition of ozone stock solution. Finally, the concentration of the catalyst was 2 g/L. The suspension was continuously magnetically stirred for half an hour and then dried overnight at 333 K. The infrared spectrum of the dry samples supported on KBr pellets, was recorded on a Nicolet 5700 FTIR spectrophotometer. The spectrum of pure KBr pellet was used as background while recording sample spectra.

In situ ATR-FTIR spectroscopy. To prepare an ATR sample, a desired amount of catalyst particles was added to D_2O solvent and the suspensions were sonicated intermittently over 48 h. And then the solid was separated by centrifugation and treated again with another aliquot of D_2O without or with IBU compound to eliminate residual H_2O. For the ozonation experiments, the ozone D_2O solution (3 mg/L) was added. The suspension was vigorously shaken, and the aliquots were immediately withdrawn for ATR-FTIR analysis. All manipulations are performed under nitrogen atmosphere when D_2O is employed. A short time before running the spectra, the samples are centrifuged, half of the supernatant is used as reference, the solid resuspended in the other half and used as the sample. The final concentration of the catalyst was 100 g/L. ATR-FTIR spectra were recorded using a Nicolet 5700 infrared spectrometer with a deuterated triglycine sulfate (DTGS) detector and a ZnSe horizontal ATR cell. Infrared spectra over the 4000–650 cm^{-1} range were obtained by averaging 32 scans with a resolution of 4 cm^{-1} at room temperature (298 K).

2.4. Procedures and analysis

Semi-batch experiments were carried out with the 1.2 L reactor as described in the previous work [25]. The reaction temperature was maintained at 20 °C. In a typical experiment, 1 L aqueous suspensions of PhACs at various concentrations and 1.5 g catalyst powders were placed in the reactor. The solution was continuously magnetically stirred, and 30 mg gaseous O_3/L oxygen–ozone was bubbled into the reactor through the porous plate of the reactor bottom at a 12 L/h flow rate. Ozone was generated by a laboratory ozonizer (DHX-SS-IG; Harbin Jiujiu Electrochemistry Technology, Harbin City, China) in the reactor. The residual ozone in the off-gas was adsorbed by a KI solution. At given time intervals, samples were withdrawn and filtered through a filter (pore size 0.45 μm; Millipore, Billerica, MA) for analysis. An aliquot of 0.1 M $Na_2S_2O_3$ was subsequently added to the sample to quench the aqueous ozone remaining in the reaction solution. The gaseous ozone concentration was measured using the iodometric titration method. The concentration of ozone dissolved in the aqueous phase was determined using the indigo method. The concentration of each PhAC was measured using high-performance liquid chromatography (1200 series; Agilent, Santa Clara, CA) with an Eclipse XDB-C18 column (5 μm, 4.6 mm × 150 mm; Agilent). The mobile phase was a solution of 60/40 (v/v) acetonitrile–phosphate buffer solution (20 mM, pH 2.5) with a flow rate of 1 mL/min. The amount of Fe^{3+} in the supernatant was measured by inductively coupled plasma optical emission spectrometry (ICP-OES) on an OPTIMA

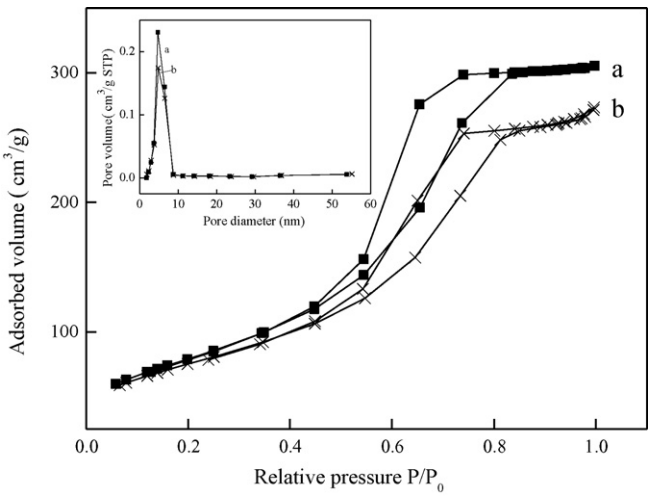

Fig. 1. Nitrogen adsorption–desorption isotherms of (a) MA and (b) β-FeOOH/MA. The inset shows the pore size distribution calculated from their desorption branch.

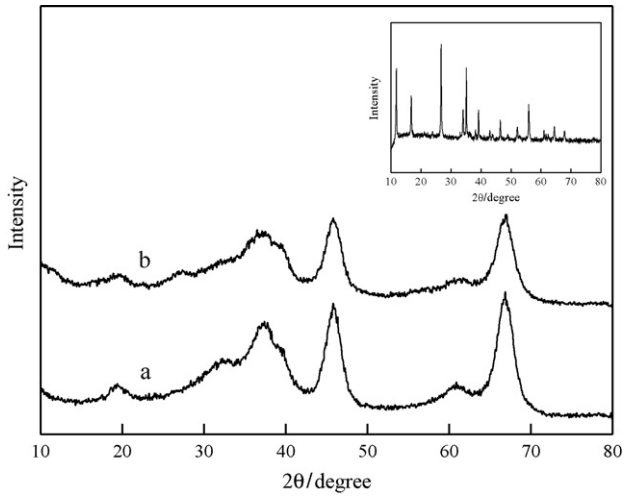

Fig. 2. XRD patterns of different catalysts: (a) MA, (b) β-FeOOH/MA. The inset shows the XRD pattern of β-FeOOH.

2000 (PerkinElmer Co.) instrument. The total organic carbon (TOC) content of the solution was analyzed using a Phoenix 8000 TOC analyzer.

3. Results and discussion

3.1. Characterization of catalysts

The nitrogen adsorption/desorption curves are presented in Fig. 1. Both MA and β-FeOOH/MA samples exhibited adsorption isotherms of type IV with hysteresis loops, which means that the materials had a mesoporous structure. The pore size distribution of β-FeOOH/MA catalyst was nearly identical to that of the MA (the inset of Fig. 1). The BET surface areas were 287 and 272 m^2/g for MA and β-FeOOH/MA, respectively. The introduction of β-FeOOH did not change significantly the pore diameters of MA and the BET surface area, indicating that β-FeOOH had high dispersion on MA. The XRD patterns of different samples are shown in Fig. 2. It has been verified that the support MA had a mesoporous structure, assigned to γ-Al_2O_3 [25]. β-FeOOH is the predominant phase of the unsupported sample prepared by hydrolysis of $FeCl_3$ under the given experimental condition (the insert of Fig. 2), while no XRD

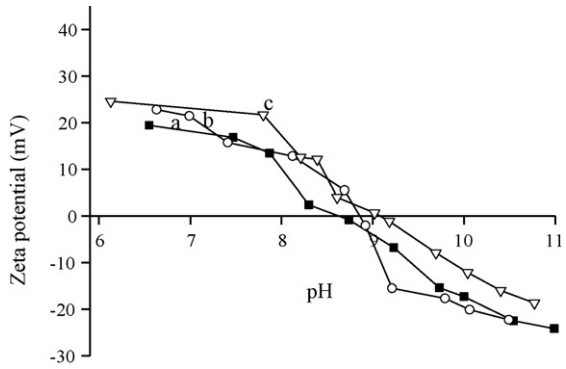

Fig. 3. Plot of the zeta potential as a function of pH for different catalyst suspensions in the presence of KNO_3 (10^{-3} M): (a) MA, (b) β-FeOOH, (c) β-FeOOH/MA.

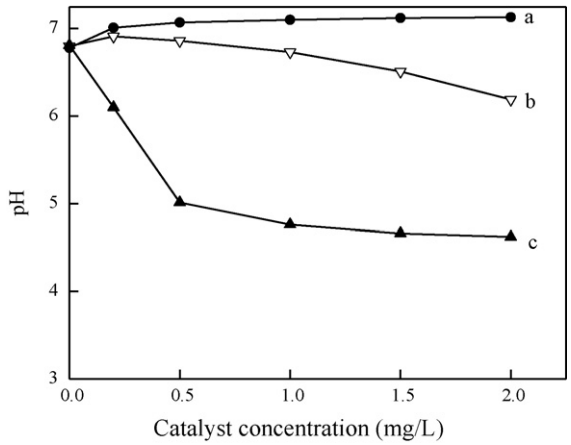

Fig. 4. pH change of solution with the addition of different catalysts: (a) MA, (b) β-FeOOH, (c) β-FeOOH/MA.

diffraction peaks of β-FeOOH were observed in the supported sample. This presumably contributed to its low loading content (3 wt%) and high dispersion on MA. Based on the same method of preparation, the supported iron oxide should have the same structure as the unsupported one. Therefore, the supported sample was designated β-FeOOH/MA.

Fig. 3 shows the changes of the zeta potential with the pH of the solution. The pH of points of zero charge (pHpzc) were 9.1, 8.8 and 8.5 for β-FeOOH/MA, β-FeOOH and MA, respectively. The three metal oxides can behave as cation or anion exchangers, which are based on the ability of surface hydroxyl groups to dissociate or to be protonated.

$$Me - OH + H^+ \Leftrightarrow Me - OH_2^+, \quad K_1^{\text{int}}$$

$$Me - OH + OH^- \Leftrightarrow Me - O^- + H_2O \quad K_2^{\text{int}}$$

where K_1^{int} and K_2^{int} are the intristic ionization constants. The pHpzc depends on ionization reactions and is related to the ionization constants [26].

$$\text{pHpzc} = 0.5\,(\text{p}K_1^{\text{int}} + \text{p}K_2^{\text{int}})$$

Upward shifts of the pHpzc for β-FeOOH/MA indicated that the catalyst surface enhanced the ability of ionizing H^+ ions, further suggesting that the surface Lewis acid sites increased. As shown in Fig. 4, the pH of aqueous β-FeOOH/MA suspension decreased with its concentration increasing. The pH of suspension was 4.64 at the catalyst concentration 2 g/L. For β-FeOOH and MA, the pH of suspension did not greatly change and tended to 6–7 with the

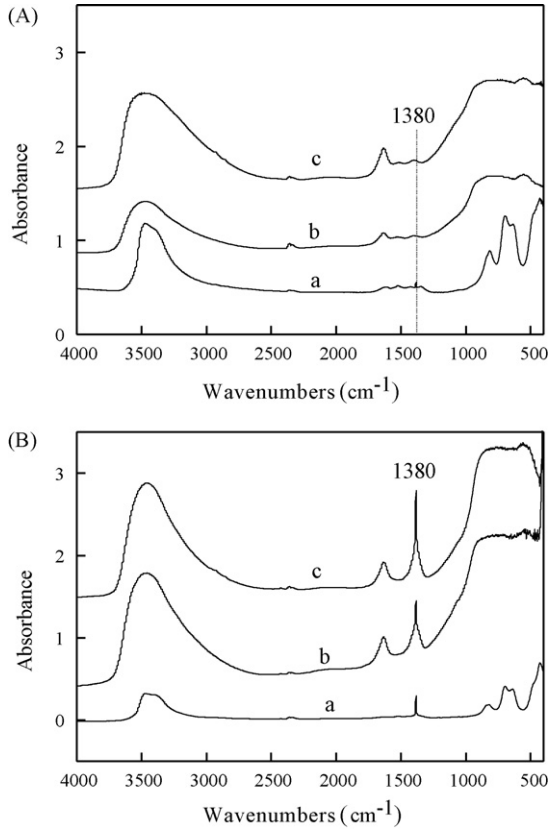

Fig. 5. FTIR spectra of various processes: (A) unozonated samples, (B) after treatment with ozone solution. For all panels, (a) β-FeOOH, (b) MA and (c) β-FeOOH/MA.

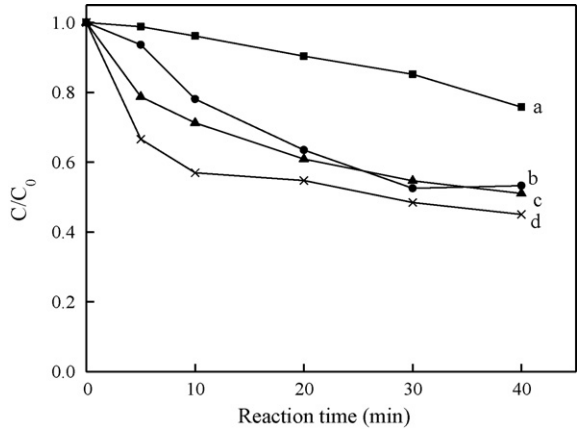

Fig. 6. Decomposition of ozone in aqueous dispersions of various catalysts: (a) without catalyst, (b) β-FeOOH, (c) MA, (d) β-FeOOH/MA.

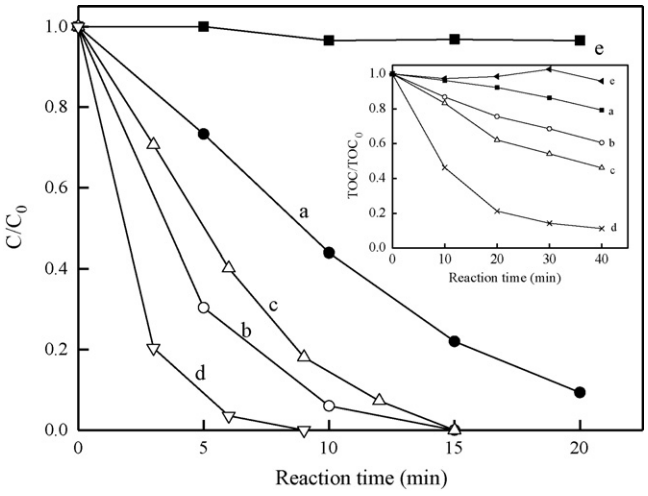

Fig. 7. Degradation of IBU in aqueous dispersions of various catalysts with ozone: (a) ozone alone, (b) β-FeOOH, (c) MA, (d) β-FeOOH/MA and (e) adsorption on β-FeOOH/MA (pH 7.0, catalyst = 1.5 g/L, gaseous ozone concentration = 30 mg/L). The inset shows the TOC removal under the corresponding conditions.

concentrations of catalysts increasing. The result indicated that β-FeOOH/MA surface had stronger Lewis acid sites than the other two. β-FeOOH/MA could have more adsorption of Lewis base such as water and ozone. The surface changes of the three catalysts were characterized by FTIR after treated with water or ozone aqueous solution. The samples for FTIR were prepared by drying catalyst suspensions with or without ozone overnight in air at 333 K. As shown in Fig. 5A, the uptake of water by β-FeOOH/MA significantly increased as indicated by the growth of the adsorbed water features which extend from approximately 3800 to 2600 cm^{-1}, compared with those on MA and β-FeOOH. Correspondingly, on the FTIR spectra of these catalysts treated with ozone aqueous solution a new peak appeared at around 1380 cm^{-1} (Fig. 5B). The same feature peak produced by the treatment of alumina with ozone was observed by Roscoe and Abbatt [27]. They verified in detail that the peak contributed to a surface oxide species formed by the interaction of ozone with Lewis acid sites on the alumina surface, and that the presence of water strongly inhibited the formation of the spectral feature at 1380 cm^{-1}. However, in the present experiment, the peak at 1380 cm^{-1} appeared after the ozone suspension was dried at 333 K overnight. The residual water in the sample did not affect the peak forming although water not ozone would hold on Lewis acid sites. The results indicated that different processes occurred in the tested conditions from the ones reported by Roscoe, which would be illustrated by in situ ATR-FTIR studies in the following. The intensities of the peak increased according to the following order: β-FeOOH/MA > MA > β-FeOOH, which closely paralleled the surface Lewis acid sites of the different catalysts. The results suggested that the surface Lewis acid sites should be relative to the peak formation of 1380 cm^{-1}. Meanwhile, a series of ozone decomposition experiments were carried out in the presence of the studied catalysts. As can be seen from Fig. 6, the ozone decomposition rate was enhanced by different catalysts, MA and β-FeOOH showed similar activity, β-FeOOH/MA exhibited the higher activity than the others. Since the decomposition of O_3 is a chain reaction. The reactive species generated from the decomposition of O_3 were not consumed due to the absence of pollutant in the experiments, leading to the rate difference to be smaller for the O_3 decomposition. However, the β-FeOOH/MA exhibited highest activity agreeing with the observation of FTIR, verifying the surface Lewis acid sites responsible for the catalytic decomposition of ozone.

3.2. Catalytic ozonation of IBU and CPFX

The catalytic activity of various catalysts was evaluated by the degradation of IBU (10 mg/L) with ozone at an initial pH 7. As shown in Fig. 7, IBU was completely degraded in β-FeOOH/MA suspension within a reaction time of 9 min, while about 80% of IBU was removed over MA and β-FeOOH, respectively, and only 50% of IBU was removed with ozone alone at the same reaction time. In addition, about 5% of IBU was adsorbed onto β-FeOOH/MA when the adsorption reached equilibrium. The pK_a of IBU is 4.9; most of IBU was in its anion form at the tested neutral pH. Meanwhile, at a reaction time of 40 min, only 20% of TOC was removed with ozone alone, while about 40 and 54% of TOC were removed in β-FeOOH and MA suspensions with ozone, respectively. In contrast, 90% of TOC were

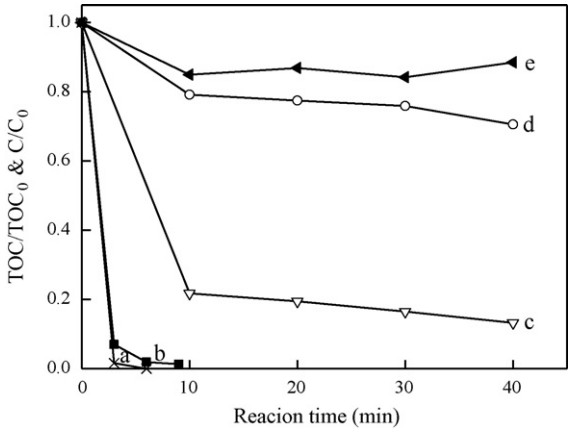

Fig. 8. Degradation of CPFX in the catalytic ozone with β-FeOOH/MA: C/C_0: (a) catalyst, (b) ozone alone; TOC/TOC_0: (c) catalyst, (d) ozone alone and (e) adsorption on catalyst (pH 7.0, catalyst = 1.5 g/L, gaseous ozone concentration = 30 mg/L).

removed over β-FeOOH/MA at the same reaction time in the inset of Fig. 7. The released Fe^{3+} concentration from β-FeOOH/MA was 11 μg/L during the ozonation reactions, which was similar to that of O_3 alone. The result indicated that the catalytic contribution of homogeneous Fe^{3+} could be neglected. β-FeOOH/MA exhibited the highest catalytic activity for the catalytic ozonation of IBU and CPFX, which paralleled with the interaction between O_3 and the catalyst, indicating the key role of surface Lewis acid sites in the catalytic oxidation of pollutants with ozone. In the meanwhile, as shown in Fig. 8, for the degradation of CPFX, the catalytic ozonation and the ozone alone exhibited similar effectiveness. However, for further degradation of intermediates, the oxidation performance of the ozone alone was not enough. Only 30% TOC was removed with ozone alone at 40 min, while 88% TOC was removed in β-FeOOH/MA suspension with ozone, indicating β-FeOOH/MA more effective for the mineralization of CPFX. Moreover, the adsorption of CPFX was examined onto β-FeOOH/MA, 12% of TOC was adsorbed. The pK_a of CPFX is 6.27 and 8.87, it was mainly in undissociated form at the tested pH. Therefore, the contribution of the adsorption was not predominant during the catalytic ozonation of IBU and CPFX.

3.3. Catalytic ozonation mechanism of β-FeOOH/MA

All the above results proved that the high efficiency of β-FeOOH/MA catalytic ozonation resulted from its comparatively strong surface Lewis acid sites. Furthermore, in situ ATR-FTIR experiments were carried out under different reaction conditions to investigate the role of the surface Lewis acid sites of the catalysts in aqueous phase. In this experiment, D_2O was used as solvent instead of H_2O to separate from the bulk OH of these catalysts. As shown in Fig. 9, the stretching vibration of the hydrogen-bonded MeO–D for β-FeOOH, MA and β-FeOOH/MA were 2463, 2445, 2547 cm^{-1}, respectively. While the corresponding 2322, 2287 and 2272 cm^{-1} were assigned to the vibrations of hydrogen-bonded D_2O. The bands at around 1500 cm^{-1} also belonged to the vibration of hydrogen-bonded D_2O. Obviously, β-FeOOH/MA exhibited the biggest intensities of hydrogen-bonded MeO–D and D_2O. The result indicated that the more surface Lewis acid sites resulted in the more chemisorbed water to be formed on the surface of β-FeOOH/MA. When ozone was added to these catalyst suspensions, all the peak intensities of three catalysts increased. The results indicated that the interaction of the catalysts with O_3 aqueous solution brought about more chemisorbed water on the surface of the catalyst. Among them, the intensities of the peaks from adsorbed water on β-FeOOH/MA were strongest indicating the greatest interaction of O_3 with it. With the addition of IBU to the reaction system,

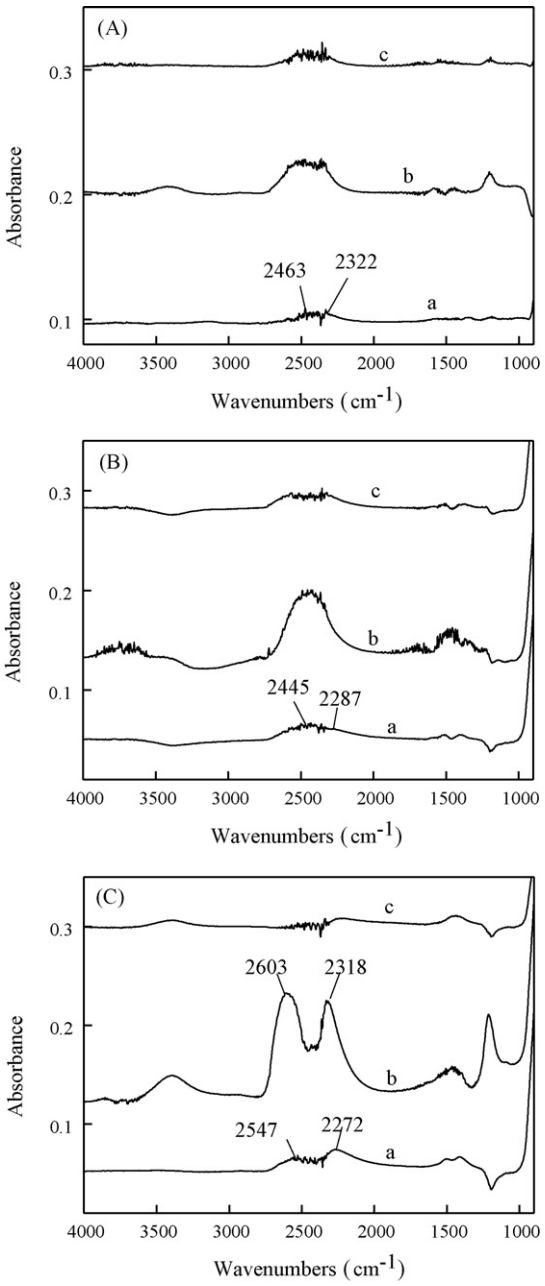

Fig. 9. ATR-FTIR spectra of different reactions in D_2O under various conditions: (A) β-FeOOH, (B) MA and (C) β-FeOOH/MA. For all panels, (a) catalyst, (b) catalyst + O_3, (c) catalyst + O_3 + IBU.

the intensities of all the peaks decreased. In the meanwhile, the degradation of IBU was also observed. The observation paralleled in their catalytic activity for the catalytic ozonation of IBU. These results indicated that the chemisorbed water and its dissociative hydroxyl groups were active precursor in the degradation of IBU. Its formation and activation depended on the surface Lewis acid sites of the catalysts. Since phosphate is a harder Lewis base than water, its existence would inhibit the adsorption of water on the Lewis acid sites of the catalyst, causing lower activity. To ascertain the conjecture, the effect of phosphate on the catalytic degradation of IBU was investigated in β-FeOOH/MA suspension with ozone. Obviously, the absorption bands of hydrogen-bonded MeO–D and D_2O disappeared in the presence of phosphate, while two new peaks appeared at 1022 and 1105 cm^{-1}, belonging to phosphate vibrations [28] as shown in Fig. 10. Accordingly, the TOC removal

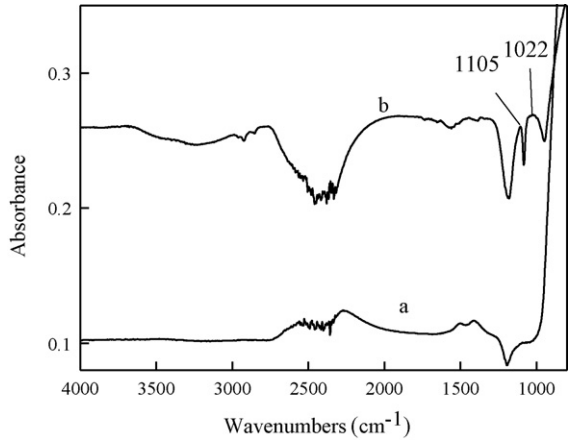

Fig. 10. ATR-FTIR spectra of β-FeOOH/MA suspension in D_2O: (a) without phosphate and (b) in the presence of 30 mM phosphate.

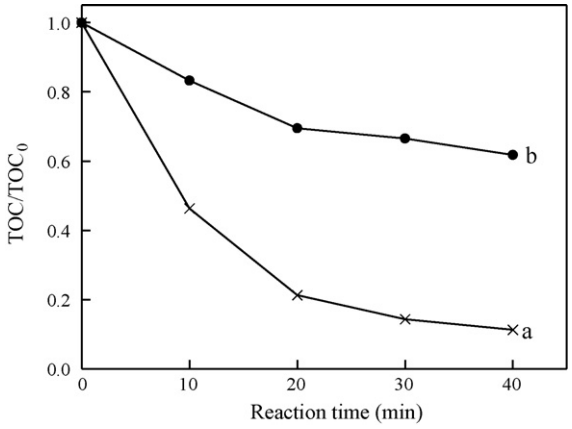

Fig. 11. Effect of phosphate on the reaction activity of β-FeOOH/MA: (a) without phosphate and (b) 5 mM phosphate (pH 7.0, catalyst = 1.5 g/L, gaseous ozone concentration = 30 mg/L).

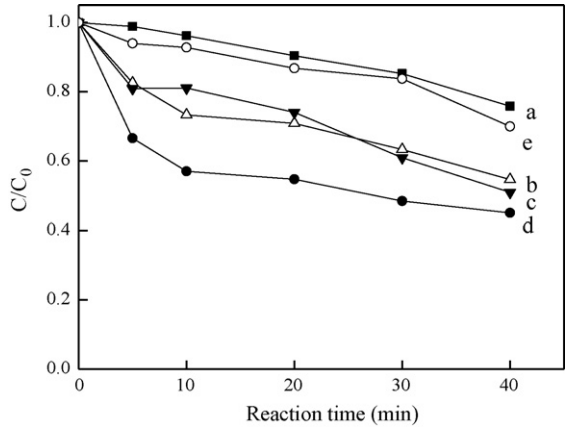

Fig. 12. Effect of phosphate on decomposition of ozone under different conditions: (a) without catalyst and phosphate, (b) with 5 mM phosphate, (c) β-FeOOH/MA with 5 mM phosphate, (d) β-FeOOH/MA, (e) with 1 M phosphate.

was greatly depressed in the presence of 5 mM phosphate (Fig. 11). Phosphate had two roles to affect the reactivity of the catalyst. One is that phosphate held the surface Lewis acid sites on the catalyst preventing chemisorption of the water, leading to lower activity, the other is that phosphate could trap •OH competing with pollutant. In order to express the former, the decomposition of O_3 was examined with and without phosphate in the absence of pollutant. As can be seen from Fig. 12, the catalytic decomposition rate of O_3 greatly decreased in the presence of phosphate, which is similar to the one in ozone alone with phosphate. The results indicated that the catalytic decomposition of O_3 was nearly completely depressed in the presence of phosphate. In addition, the decomposition of O_3 belonged to the chain reaction, producing free radicals, which could be scavenged by the radical scavenger and organics, thus accelerating the decomposition of O_3 [29,30]. The observation of the phosphate at 5 mM enhancing the decomposition rate of O_3 in pure water is different from those reported [29]. However, with the increasing phosphate concentration, the decomposition rate of O_3 decreased. In these experiments with different phosphate concentrations, the solution pH was kept at pH 7 by adjusting the addition ratio of Na_2HPO_4 and NaH_2PO_4. The formation of phosphate in water mainly depended on solution pH. Therefore, the characters of phosphates in these experiments were same although their concentrations were different. For the O_3 decomposition experiment in pure water, the initial pH 7 of solution was adjusted by 0.1 M NaOH solution, and the solution pH was about 7.5 after the reaction finished, so the pH changes favored the decomposition of O_3. The interaction of phosphate with ozone still needs to be investigated further in detail in another work. Nevertheless, it was obvious that the catalyst hardly played any role in the decomposition of O_3 in the presence of phosphate compared with the one in ozone alone with phosphate. The results indicated that the catalytic role of β-FeOOH/MA was almost completely depressed due to the replacement of surface hydroxyl group and chemisorbed water by phosphate. These studies confirm that the reactive oxygen species are generated by the interaction of the ozone in aqueous solution with the surface hydrogen-bonded MeO–D and D_2O in aqueous phase catalytic ozonation, while the surface Lewis acid sites are reactive sites for the surface hydroxylation of catalysts in water. Therefore, the peak at 1380 cm^{-1} shown in Fig. 5B was formed from the interaction of the hydroxyl groups and the chemisorbed water with O_3. Zhao et al. [20] studied the relationship of the density of surface–OH_2^+ and the zero charge point of the pH of catalyst and the •OH formation, indicating the initiation of •OH by the interaction of ozone in aqueous solution with the surface–OH_2^+. Here, the studies of in situ ATR-FTIR supplied direct evidences for the interaction of the Lewis acid sites with H_2O, the surface hydrogen-bonded MeO–D and D_2O with O_3 at the solid–liquid interface, proving the process of catalytic ozonation.

4. Conclusions

Surface Lewis acid sites on β-FeOOH/MA were more greatly enhanced by the combination of β-FeOOH and MA. The catalyst showed high efficiency for the mineralization of IBU and CPFX aqueous solution with ozone. In situ ATR-FTIR studies verified that the dissociative chemisorptions of D_2O occurring at the surface Lewis acid sites of the catalyst, and interacted with ozone to initiate ROS. The stronger Lewis acid sites of β-FeOOH/MA caused the more chemisorbed water enhancing the interaction with ozone, resulting in higher catalytic reactivity. The observations verified that the Lewis acid sites were reactive center for the catalytic ozonation of PhACs in water.

Acknowledgments

This work was supported by the National Natural Science Foundation of China (No. 20977104, 50778169, 50921064) and the Chinese Academy of Sciences (kzcx1-yw-06-02) and the 973 project (2010CB933600).

Appendix A. Supplementary data

Supplementary data associated with this article can be found, in the online version, at doi:10.1016/j.apcatb.2010.04.014.

References

[1] B. Halling-Sørensen, S. Nors Nielsen, P.F. Lanzky, F. Ingerslev, H.C. Holten Lützhøft, S.E. Jørgensen, Chemosphere 36 (1998) 357–393.
[2] N.M. Vieno, T. Tuhkanen, L. Kronberg, Environ. Sci. Technol. 39 (2005) 8220–8226.
[3] M.J. Benotti, B.J. Brownawell, Environ. Sci. Technol. 41 (2007) 5795–5802.
[4] T. Heberer, Toxicol. Lett. 131 (2002) 5–17.
[5] F. Pomati, A.G. Netting, D. Calamari, B.A. Neilan, Aquat. Toxicol. 67 (2004) 387–396.
[6] F. Pomati, S. Castiglioni, E. Zuccato, R. Fanelli, D. Vigetti, C. Rossetti, D. Calamari, Environ. Sci. Technol. 40 (2006) 2442–2447.
[7] T.A. Ternes, M. Meisenheimer, D. McDowell, F. Sacher, H.J. Brauch, B. Haist-Gulde, G. Preuss, U. Wilme, N. Zulei-Seibert, Environ. Sci. Technol. 36 (2002) 3855–3863.
[8] P.E. Stackelberg, E.T. Furlong, M.T. Meyer, S.D. Zaugg, A.K. Henderson, D.B. Reissman, Sci. Total Environ. 329 (2004) 99–113.
[9] C. Zwiener, F.H. Frimmel, Water Res. 34 (2000) 1881–1885.
[10] N.M. Vieno, H. Harkki, T. Tuhkanen, L. Kronberg, Environ. Sci. Technol. 41 (2007) 5077–5084.
[11] M.M. Huber, S. Canonica, G.-Y. Park, U. von Gunten, Environ. Sci. Technol. 37 (2003) 1016–1024.
[12] B. DeWitte, J. Dewulf, K. Demeestere, V. Van De Vyvere, P. De Wispelaere, H. Van Langenhove, Environ. Sci. Technol. 42 (2008) 4889–4895.
[13] R. Andreozzi, A. Insola, V. Caprio, R. Marotta, V. Tufano, Appl. Catal. A: Gen. 138 (1996) 75–81.
[14] B. Legube, N. Karpel Vel Leitner, Catal. Today 53 (1999) 61–72.
[15] F.J. Beltrán, F.J. Rivas, R. Montero-de-Espinosa, Appl. Catal. B: Environ. 47 (2004) 101–109.
[16] W.-J. Huang, G.-C. Fang, C.-C. Wang, Colloids Surf. A: Physicochem. Eng. Aspects 260 (2005) 45–51.
[17] F.J. Beltrán, F.J. Rivas, R. Montero-de-Espinosa, Appl. Catal. B: Environ. 39 (2002) 221–231.
[18] B. Kasprzyk-Hordern, M. Zióek, J. Nawrocki, Appl. Catal. B: Environ. 46 (2003) 639–669.
[19] K.M. Bulanin, J.C. Lavalley, A.A. Tsyganenko, Colloids Surf. A: Physicochem. Eng. Aspects 101 (1995) 153–158.
[20] L. Zhao, Z.Z. Sun, J. Ma, Environ. Sci. Technol. 43 (2009) 4157–4163.
[21] P.W. Schindler, in: M.A. Anderson, A.J. Rubin (Eds.), Adsorption of Inorganics at Solid–Liquid Interfaces, Ann Arbor Publishers, Inc., Michigan, 1981, pp. 1–50.
[22] D.A. Dzombak, F.M.M. Morel, Surface Complexation Modeling, John Wiley & Sons, New York, 1990.
[23] W. Stumm, Chemistry of the Solid–Water Interface, John Wiley & Sons, New York, 1992.
[24] B.J. Xu, T.C. Xiao, Z.F. Yan, X. Sun, J. Sloan, S.L. González-Cortés, F. Alshahrani, M.L.H. Green, Micropor. Mesopor. Mater. 91 (2006) 293–295.
[25] L. Yang, C. Hu, Y.L. Nie, J.H. Qu, Environ. Sci. Technol. 43 (2009) 2525–2529.
[26] J. Nawrocki, M. Rigney, A. McCormick, P.W. Carr, J. Chromatogr. A 657 (1993) 229–282.
[27] J.M. Roscoe, J.P.D. Abbatt, J. Phys. Chem. A 109 (2005) 9028–9034.
[28] M.I. Tejedor-Tejedor, M.A. Anderson, Langmuir 2 (1986) 203–210.
[29] J. Staehelin, J. Hoigné, Environ. Sci. Technol. 16 (1982) 676–681.
[30] H. Taube, W.C. Bray, J. Am. Chem. Soc. 62 (1940) 3357–3373.